Activation of mosquito immunity blocks the development of transmission-stage filarial nematodes

Elizabeth B. Edgerton[a,1], Abigail R. McCrea[a,1], Corbett T. Berry[a,2], Jenny Y. Kwok[a,3], Letitia K. Thompson[a,4], Brittany Watson[b], Elizabeth M. Fuller[c], Thomas J. Nolan[a], James B. Lok[a], and Michael Povelones[a,5]

[a]Department of Pathobiology, University of Pennsylvania School of Veterinary Medicine, Philadelphia, PA 19104; [b]Department of Clinical Sciences & Advanced Medicine, University of Pennsylvania School of Veterinary Medicine, Philadelphia, PA 19104; and [c]Shelter Medicine, Charleston Animal Society, North Charleston, SC 29406

Edited by Carolina Barillas-Mury, National Institutes of Health, Bethesda, MD, and approved January 2, 2020 (received for review May 31, 2019)

Mosquito-borne helminth infections are responsible for a significant worldwide disease burden in both humans and animals. Accordingly, development of novel strategies to reduce disease transmission by targeting these pathogens in the vector are of paramount importance. We found that a strain of *Aedes aegypti* that is refractory to infection by *Dirofilaria immitis*, the agent of canine heartworm disease, mounts a stronger immune response during infection than does a susceptible strain. Moreover, activation of the Toll immune signaling pathway in the susceptible strain arrests larval development of the parasite, thereby decreasing the number of transmission-stage larvae. Notably, this strategy also blocks transmission-stage *Brugia malayi*, an agent of human lymphatic filariasis. Our data show that mosquito immunity can play a pivotal role in restricting filarial nematode development and suggest that genetically engineering mosquitoes with enhanced immunity will help reduce pathogen transmission.

mosquito | immunity | *Dirofilaria* | *Brugia* | Malpighian tubule

Mosquito-borne filarial nematode infections are responsible for a significant worldwide disease burden in both humans and animals. Canine heartworm, a zoonotic disease caused by *Dirofilaria immitis*, is one of the most debilitating parasitic diseases of companion animals (1, 2). Moreover, infection by *Wuchereria bancrofti*, *Brugia malayi*, and *Brugia timori* cause an estimated 120 million cases of human lymphatic filariasis (3). Current control methods for these diseases focus on treatment of the infected vertebrate host. However, mosquitoes function as both vectors and intermediate hosts of filarial nematodes, making them attractive targets for transmission-blocking interventions.

During an infection cycle, microfilariae that are circulating in a vertebrate host are taken up by mosquitoes during blood feeding. In an infection-susceptible vector, ingested parasites then migrate out of the blood meal to specific tissues. In the case of *D. immitis*, microfilariae migrate posteriorly out of the bloodmeal, into the midgut surroundings, and enter the lumen of the Malpighian tubules, the mosquito renal organ, where they eventually enter principal cells (*SI Appendix*, Fig. S1*A*). In the case of *B. malayi*, microfilariae penetrate the midgut wall, migrate through the hemocoel, and enter cells of the indirect flight muscles in the thorax (*SI Appendix*, Fig. S1*B*). In their respective sites of development, the parasites undergo two larval molts, ultimately developing into infectious third-stage larvae over a period of ∼2 wk. Larvae then migrate to the labial sheath of the mosquito proboscis, where heat and other factors encountered during blood feeding stimulate these transmission-stage larvae to emerge from the labellum, located at the extreme tip of the labium (4, 5). Larvae are deposited on the skin in a drop of hemolymph and can enter the vertebrate host through the bite wound, completing the infection cycle (5).

Mosquito species and strains vary in their capacity to support filarial worm development. In some populations, such as *Aedes aegypti*, both infection-susceptible and infection-refractory traits can cocirculate, and can be used to select pure-breeding lines (6, 7). The *Ae. aegypti* model has been used extensively to study mechanisms of refractoriness (8–15). In refractory strains, microfilariae migrate to and enter the appropriate cells for larval development but fail to develop (13, 16–18). Transplantation studies between susceptible and refractory mosquitoes using *D. immitis*-infected Malpighian tubules showed that susceptibility is autonomously determined by the tubules (17).

While both susceptible and refractory strains of *Ae. aegypti* activate immune signaling during infection with *B. malayi* (19, 20), infection of susceptible *Ae. aegypti* with immunostimulatory strains of *Wolbachia* or inoculation of bacteria into the hemolymph reduces the number of transmission-stage filariae (21, 22), suggesting that increased immune responses of mosquito vectors may reduce transmission of filarial nematodes. In support, data presented here demonstrate that susceptible *Ae. aegypti* fail to mount a robust immune response during filarial infection, and that genetically augmenting mosquito immunity can block the development of transmission stages of both *D. immitis* and *B. malayi*.

Significance

Infections with filarial nematodes, resulting from the bite of an infected mosquito, have a huge health impact worldwide. Sequencing mosquito transcripts revealed that a strain of *Aedes aegypti* that is refractory to infection with heartworm robustly activates immune genes, compared to a susceptible strain. These differences were detected early in infection and in the tissue important for larval development. Using a new assay, we found that bolstering mosquito immune activation through knockdown of a negative regulator resulted in a strong block in the emergence of transmission-stage filarial larvae, including those that cause human lymphatic filariasis. This work provides opportunities to block pathogen transmission by targeting filarial nematodes in the mosquito vector.

Author contributions: E.B.E., A.R.M., J.B.L., and M.P. designed research; E.B.E., A.R.M., J.Y.K., L.K.T., and M.P. performed research; C.T.B., B.W., and E.M.F. contributed new reagents/analytic tools; E.B.E., A.R.M., C.T.B., J.Y.K., L.K.T., T.J.N., J.B.L., and M.P. analyzed data; and A.R.M., T.J.N., J.B.L., and M.P. wrote the paper.

The authors declare no competing interest.

This article is a PNAS Direct Submission.

Data deposition: Data submitted to Gene Expression Omnibus (GEO), under accession number accession no. GSE142155.

[1]E.B.E. and A.R.M. contributed equally to this work.

[2]Present address: School of Biomedical Engineering, Science and Health Systems, Drexel University, Philadelphia, PA 19104.

[3]Present address: Surgery Department, VCA Animal Specialty Group, Los Angeles, CA 90039.

[4]Present address: Department of Microbiology, New York University School of Medicine, New York, NY 10016.

[5]To whom correspondence may be addressed. Email: mpove@vet.upenn.edu.

This article contains supporting information online at https://www.pnas.org/lookup/suppl/doi:10.1073/pnas.1909369117/-/DCSupplemental.

First published February 3, 2020.

Results

Refractory Mosquitoes Activate a Stronger Immune Response to Filarial Infection than Susceptible Mosquitoes. For these studies, we assessed the fate of ingested *D. immitis* microfilariae in susceptible and refractory strains of *Ae. aegypti*, referred to hereafter as *Ae. aegypti*^{S} and *Ae. aegypti*^{R}, respectively. Notably, although these laboratory strains were established in the 1970s, the genetic region controlling susceptibility to filarial infection in populations of recently collected Kenyan *Ae. aegypti* maps to the same locus as in these laboratory strains (20), supporting their use as a model system. In susceptible mosquitoes, larvae develop and morphologically transform from long slender microfilariae to short, "sausage-form" first-stage larvae. In the refractory strain, this development is blocked, and parasites retain a microfilaria-like morphology and do not develop further (Fig. 1*A*). In support of our morphological observations, we found that the number of *D. immitis* transcripts detected in *Ae. aegypti*^{S} Malpighian tubules increased at days 2 and 3 postinfection compared to *Ae. aegypti*^{R} (*SI Appendix*, Fig. S2). This indicates that microfilariae arrive at the appropriate tissue, but that development is arrested in the refractory strain.

Based on these observations, we sought to determine the molecular basis of resistance to *D. immitis* infection by comparing the transcriptional responses of infected *Ae. aegypti*^{S} and *Ae. aegypti*^{R} Malpighian tubules. Three days postinfection, there is a strong difference in the transcriptional responses of refractory and susceptible mosquitoes, with 1,573 genes that are differentially regulated by twofold or greater. Of these, 924 genes are up-regulated and 649 are down-regulated (Fig. 1*B*). Since immune response genes were previously found to be differentially regulated in these strains during infection by *B. malayi*, we examined a set of 319 predicted immune genes (23) and found that 21.3% (68 genes) were differentially regulated in *D. immitis*-infected *Ae. aegypti*^{R} Malpighian tubules as compared to *Ae. aegypti*^{S}. Of these, the majority were up-regulated, 88.2% (60/68) compared to 11.8% (8/68) that were down-regulated.

To further explore immune gene transcriptional responses between our strains, both before and throughout the course of infection, we used Gene Set Enrichment Analysis (GSEA) (24, 25). Six gene sets were analyzed, including 1) predicted immune genes, genes up-regulated by 2) Toll, 3) immune deficiency (IMD) (26), or 4) Janus Kinase Signal Transducers and Activators of Transcription (JAK-STAT) (27) signaling, and genes that are up-regulated when mosquitoes are infected with 5) *B. malayi* (20) or 6) *Wolbachia* (28). Despite baseline differences in global gene expression between the two strains, none of the immune or infection gene sets were enriched in a strain-specific manner (*SI Appendix*, Fig. S3*A* and Table S2). In contrast, at day 3 postinfection, all gene sets except those induced by JAK-STAT are significantly enriched in *Ae. aegypti*^{R} compared to infected *Ae. aegypti*^{S} (Fig. 1*B* and *SI Appendix*, Table S2). This analysis also reveals that immune genes and immune pathway target genes are strongly activated in Malpighian tubules following *D. immitis* infection. We found that all gene sets, except those induced by JAK-STAT, were highly enriched following infection compared to the baseline control in both *Ae. aegypti*^{R} (*SI Appendix*, Fig. S3*C* and Table S2) and *Ae. aegypti*^{S} (*SI Appendix*, Fig. S3*D* and Table S2). However, our data suggest that, while both strains respond to infection by up-regulating immune genes, the refractory strain mounts a stronger response. Indeed, when we examined the 76 immune genes that are differentially regulated in either strain during the time course of infection, the largest cluster comprises 53 (69.7%) genes that are more robustly up-regulated in the refractory strain compared to the susceptible strain (Fig. 1*C*). Within this group of 53 genes, 41.5% are targets of Rel1 or Rel2 (Fig. 1*C*), implicating Toll and IMD signaling in the transcriptional response to *D. immitis* infection. In support of this, analysis of the expression of signal transduction machinery of the Toll, IMD, and JAK-STAT pathways in *Ae. aegypti*^{R} and *Ae. aegypti*^{S} mosquitoes indicates that the core components for all three are expressed by Malpighian tubules in both strains and most are not differentially regulated (*SI Appendix*, Fig. S4). This suggests that differences in the immune responses between the strains or failure of either strain to elicit JAK-STAT targets is due to differences in pathway activation and not because of gross differences in expression of signal transduction components.

Activation of Mosquito Toll Pathway Blocks Emergence of *D. immitis* Third-Stage Larvae. Failure to induce strong activation of immune genes in the susceptible strain could result from an inability to detect or respond to *D. immitis* or increased tolerance to infection driven by enhanced sensitivity to immune evasive molecules produced by early developmental stages of *D. immitis*. In either case, we hypothesized that artificial activation of immune signaling in *Ae. aegypti*^{S} would make them refractory to infection.

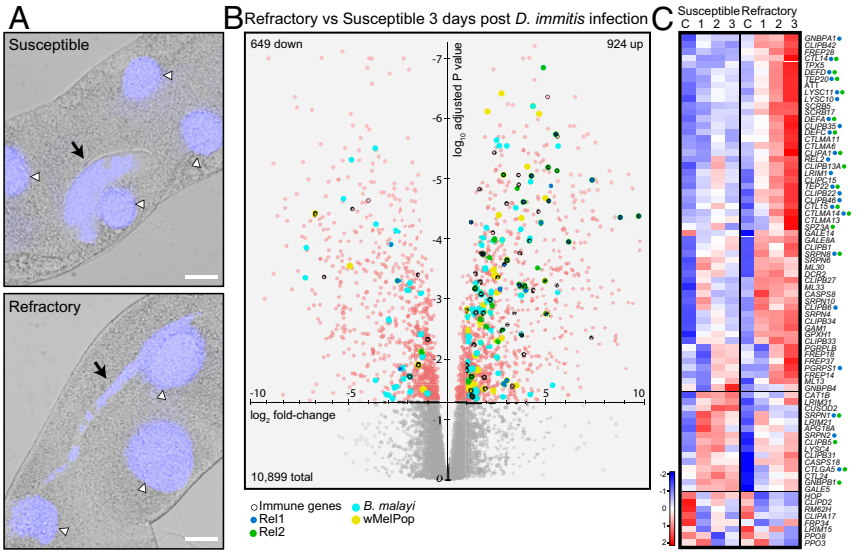

Fig. 1. Immune genes are more robustly up-regulated in *D. immitis*-infected Malpighian tubules of refractory *Ae. aegypti* compared to an infection susceptible strain. (*A*) Overlay of light and fluorescent photomicrographs of representative portions of *Ae. aegypti*^{S} (Susceptible) and *Ae. aegypti*^{R} (Refractory) Malpighian tubules containing *D. immitis* (arrows) 3 d postinfection. The nuclei of tubule principal cells, stained with Hoechst, are indicated with white arrowheads. (Scale bar, 25 μm.) (*B*) Volcano plot showing differentially regulated genes in Malpighian tubules of *Ae. aegypti*^{R} compared to *Ae. aegypti*^{S} 3 d post *D. immitis* infection. Different color dots indicate members of Immune (open), Rel1 up-regulated (blue), Rel2 up-regulated (green), or up-regulated by *B. malayi* (cyan) or by *Wolbachia* infection (yellow) gene sets that contribute to significant GSEA scores. Dots appearing with more than one color are present in multiple lists. Panel *B* appears in high resolution format in *SI Appendix*, Fig. S3*B*. (*C*) Clustered heat map of differentially expressed immune genes in either *Ae. aegypti*^{S} (Susceptible) or *Ae. aegypti*^{R} (Refractory) Malpighian tubules 3 d post *D. immitis* infection relative to its uninfected control. The key indicates the row z score, with red corresponding to up-regulated, white corresponding to neutral, and blue corresponding to down-regulated relative to its control. Horizontal lines separate three distinct clusters of expression profiles. Dots indicate genes that are known targets of Rel1 (blue) or Rel2 (green).

To test this, we used an assay to quantify transmission-stage larvae capable of emerging from individual mosquitoes. We examined the effect of activating either the Toll or IMD pathways by silencing the pathway-specific negative regulators Cactus and Caspar, respectively. We found that activation of the Toll pathway prior to infection not only reduced transmission-stage larvae, but that it also had a modest effect on the number of ingested worms (*SI Appendix*, Fig. S5). Therefore, we revised our protocol by performing gene silencing after mosquitoes fed on *D. immitis*-infected blood. Specifically, a large group of untreated mosquitoes was infected with *D. immitis* and then blindly divided into groups for injection with ds*Cactus*, ds*Caspar*, or control ds*GFP*, ensuring even uptake of worms between the groups (Fig. 2*A*). Treatment with ds*Cactus* led to a highly significant reduction in the prevalence of mosquitoes with emerging transmission larvae and in the number of transmission-stage larvae emerging from individual mosquitoes compared to the control or ds*Caspar*-treated mosquitoes (which did not differ from each other; Fig. 2 *B* and *C*). We did observe, however, a fitness cost to the mosquitoes associated with Toll pathway activation (*SI Appendix*, Fig. S6), which has been reported previously in both *Aedes* and *Anopheles* and is independent of infection (19, 29). To test whether the effects of Toll activation were mediated through Rel1, a pathway-specific nuclear factor κB (NF-κB) transcription factor, we silenced both Cactus and Rel1 and found a complete rescue of emerging transmission-stage larvae (Fig. 2 *D* and *E* and *SI Appendix*, Fig. S7). Given that *Ae. aegypti*^{S} activate immune target genes following infection (*SI Appendix*, Fig. S3*D* and Table S2), it is somewhat surprising that silencing Rel1 alone did not lead to an increase in L3 emergence. However, because the immune genes activated in Malpighian tubules during infection are targets of both the Toll and IMD pathways, we tested whether silencing both Rel1 and Rel2, an IMD pathway-specific NF-κB transcription factor, would lead to an increase in emerging transmission-stage larvae. Consistent with our previous results, silencing either alone did not change the outcome of infection. Interestingly, however, when Rel1 and Rel2 were silenced together in *Ae. aegypti*^{S}, there was a modest but significant increase in the prevalence and intensity of emerging transmission-stage larvae (Fig. 2 *F* and *G* and *SI Appendix*, Fig. S8). These data suggest that the transcriptional response activated by *Ae. aegypti*^{S} following infection is functional and limits maximal infection.

Toll Pathway Activation Blocks *D. immitis* Larval Development in the Malpighian Tubules. We next determined the fate of *D. immitis* larvae in mosquitoes with activated Toll signaling. After confirming the reduction in the prevalence and number of transmission-stage larvae emerging from mosquitoes following ds*Cactus* treatment (Fig. 3 *A*–*C*), we dissected the Malpighian tubules and scored the number of larvae still present (Fig. 3*D*). We observed a larger number of developing larvae still present within the tubules in ds*Cactus*-treated mosquitoes compared to the control. To score

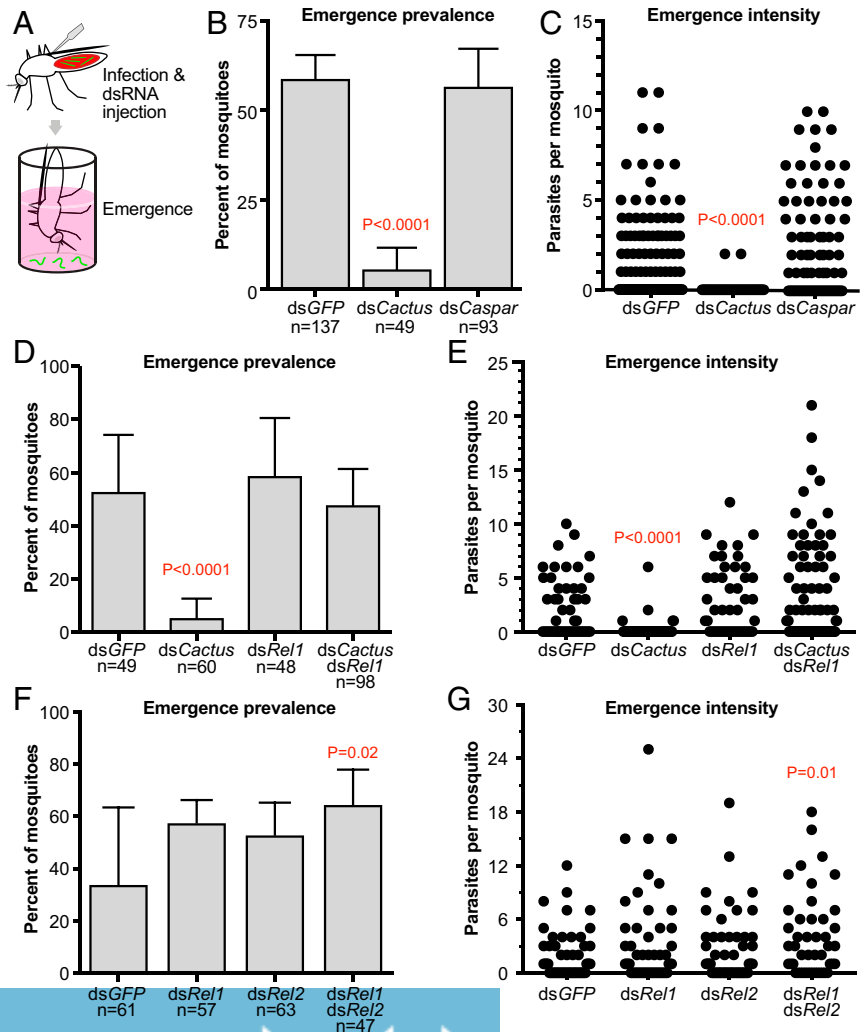

Fig. 2. Toll pathway activation reduces emerging transmission-stage *D. immitis*. (*A*) Schematic diagram of the experimental workflow where mosquitoes are infected with *D. immitis*, then immediately injected with dsRNA. (*B*) Graph of the average prevalence of emerging transmission-stage *D. immitis* larvae. The error bar indicates the SD, and the *P* value is from a χ^2 test. (*C*) Dots indicate the number of transmission-stage *D. immitis* larvae emerging from individual mosquitoes. The *P* value is from a Kruskal–Wallis test with Dunn's correction. Data in *B* and *C* are pooled from three independent experiments with ds*Cactus* and ds*Caspar* and a fourth where only ds*Cactus* was injected. (*D* and *F*) Graph of the average prevalence of individuals with at least one emerging parasite assayed 17 d postinfection. The error bar indicates the SD. The *P* value is from a χ^2 test. (*E* and *G*) Dots indicate the number of transmission-stage larvae emerging per mosquito assayed 17 d postinfection. The *P* value is from a Kruskal–Wallis test with Dunn's correction for multiple comparisons. Data in *D* and *E* and *F* and *G* are pooled from two and three independent experiments, respectively.

additional larvae present in the hemocoel, we subjected the head and remaining carcass to an emergence assay and again found that more larvae emerged from control samples than from samples treated with ds*Cactus* (Fig. 3*E*). These larvae were phenotypically similar to those that emerged in the first assay, regardless of the treatment. Pooling all larvae at all developmental stages present across all samples revealed that the ds*Cactus*-treated mosquitoes had the same total number as the controls (Fig. 3*F*). The median and range corresponded well with the median uptake and range we observe in these experiments, indicating that we are able to track the fate of the majority of microfilariae that were initially ingested (compare Fig. 3*F* and *SI Appendix*, Fig. S5). The larvae that were present in the Malpighian tubules 17 d following ds*Cactus* treatment were typically stunted, resembling early stages of *D. immitis* development. By contrast, elongated, transmission-stage larvae were more often observed in the tubules of the controls (Fig. 3*G*). We note that, although developmentally affected, the larvae in ds*Cactus*-treated mosquitoes were viable and could be observed moving in the tissue. Taken together, we find that Toll pathway activation causes the observed reduction in the number of transmission-stage larvae by effecting a block or strong delay in larval development.

Activation of Mosquito Toll Pathway Blocks Emergence of *B. malayi* Third-Stage Larvae. We next determined whether boosting the Toll pathway could also block the development of transmission-stage *B. malayi*, an agent of human lymphatic filariasis, using the same postinfection gene silencing protocol described above. Prior to injection of double-stranded RNA (dsRNA), we measured the uptake as a median of 8 microfilariae with a range from 2 to 19. Notably, there was a significant reduction in the prevalence (Fig. 4*A*) and number of emerging transmission-stage *B. malayi* per mosquito (Fig. 4*B*) following treatment with ds*Cactus*. Although the blockade of *B. malayi* development was not as strong as it was with *D. immitis*, our data nevertheless indicate that, despite their different sites of development (*SI Appendix*, Fig. S1), artificial activation of Toll signaling can inhibit the production of transmission-stage filarial larvae capable of emerging from mosquitoes.

Discussion

Previous studies have shown that the species-specific tissue sites of *D. immitis* and *B. malayi* larval development can autonomously restrict their development (30, 31). Typically, developmental restriction was coincident with larval melanization (10), a process that is important in restricting nematode infections in other insect models (32, 33). Our data reveal that activation of Toll and IMD immune pathways in Malpighian tubules is a likely mechanism contributing to this restriction. There is a strong correlation between strength of immune activation and the degree of larval restriction. In *Ae. aegypti*^{R}, the immune response is strong, and, once reaching the Malpighian tubules, the parasites do not noticeably develop. In *Ae. aegypti*^{S}, the immune response is attenuated, and the majority of ingested filariae can complete their entire life cycle, forming emerging third-stage larvae. Nevertheless, our experiments show that the immune response in *Ae. aegypti*^{S} is functional, as removing it by Rel1 and Rel2 cosilencing further increases the production of emerging transmission-stage larvae. However, filariae themselves can make mosquitoes more tolerant to infection, by inhibiting melanization (34), and, even though we do not observe melanization, it is still possible that the attenuated immune response in *Ae. aegypti*^{S} is caused by a strain-specific response to factors secreted by the developing larvae.

Interestingly, many of the immune proteins that we find to be up-regulated following infection with *D. immitis* encode secreted proteins. This is in agreement with previous studies implicating humoral immunity in restricting larval development (35–37). It also suggests that the Malpighian tubules may contribute to the immune function of the hemolymph. Although Malpighian tubules play a significant role in the humoral immune response to

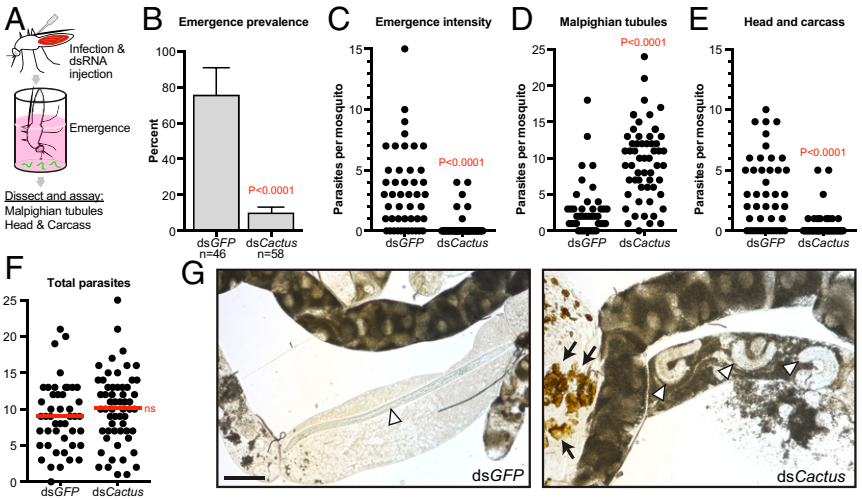

Fig. 3. Toll pathway activation blocks *D. immitis* development in Malpighian tubules. (*A*) Schematic diagram of the experimental workflow. After performing an emergence assay with whole mosquitoes, larvae were assayed in dissected Malpighian tubules. The head and carcass were placed separately into wells of a multiwell plate to capture larvae migrating in the hemocoel. (*B*) Graph of the average prevalence of emerging transmission-stage *D. immitis* larvae assayed 17 d postinfection. The error bar indicates the SD, and the *P* value is from a χ^2 test. (*C*) Dots are the number of transmission-stage *D. immitis* larvae emerging from individual mosquitoes assayed 17 d postinfection. Data are pooled from three independent experiments. (*D*) Dots indicate the number of larvae present in dissected Malpighian tubules. (*E*) Dots indicate the number of larvae emerging from the combined head and carcass following Malpighian tubule dissection. The *P* value in *C*–*E* is from a Mann–Whitney test. (*F*) Dots indicate pooled parasite numbers present across all tissues, which are normally distributed. Red lines indicate the mean. The populations are not significantly different (ns) using an unpaired *t* test with Welch's correction. (*G*) Representative images of dissected Malpighian tubules from ds*Cactus*- and ds*GFP*-treated (control) mosquitoes after performing an emergence assay. Larvae are indicated with white arrowheads. Note that the larvae in the ds*Cactus*-treated mosquitoes are typically stunted compared to the more elongated larva in the ds*GFP*-treated controls. Also indicated are deposits of melanin that appear specifically in the hindguts of some of the ds*Cactus*-treated mosquitoes. The scale for both images is the same. (Scale bar, 100 μm.)

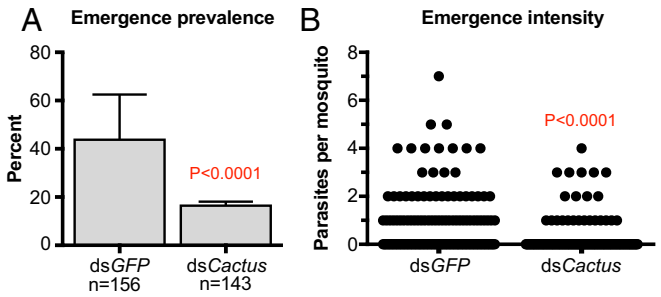

Fig. 4. Toll pathway activation reduces emerging transmission-stage *B. malayi*. (*A*) Graph of the average prevalence of emerging transmission-stage *B. malayi* larvae assayed 12 d postinfection. The error bar indicates the SD, and the *P* value is from a χ^2 test. (*B*) Dots are the number of transmission-stage *B. malayi* larvae emerging from individual mosquitoes assayed 12 d postinfection. The *P* value is from a Mann–Whitney test. Data are pooled from three independent experiments.

septic injury in *Drosophila*, little is known about their immune function in mosquitoes (38–41). As the insect renal organ, they are well positioned to surveil the hemolymph for microbial products. However, as preinfective *D. immitis* larvae are localized intracellularly, it remains to be determined whether invaded cells respond directly to the presence of the pathogen or whether the response occurs in adjacent uninfected cells. Either possibility suggests a mechanism for innate immune recognition in the site of larval development during nematode infection in insects.

Our results indicate that both Toll and IMD pathways are activated in Malpighian tubules following *D. immitis* infection. Given that these two pathways are typically triggered by distinct stimuli (42), the concurrent activation of both pathways indicates that multiple overlapping immune mechanisms are operating during infection. IMD pathway signaling is engaged following sensing of Gram-negative bacteria, suggesting that bacteria within the mosquito midgut adhere to the microfilariae surface and are subsequently carried to sites of larval development to initiate an immune response. In addition, neuropeptides secreted by the brain into the hemolymph can activate the IMD pathway in *Drosophila* Malpighian tubules through activation of the nitric oxide cascade (43, 44). In contrast, the Toll pathway is typically triggered by Gram-positive bacteria and fungi, which are also present in the mosquito midgut and thus could be carried by migrating microfilariae into other tissues. Toll signaling is used during development and tissue homeostasis and can also be activated following sensing of danger signals generated by tissue damage (45), suggesting that Toll signaling may also help tissue regeneration following damage caused by microfilariae. It will be important to test whether the difference in the strength of immune activation in *Ae. aegypti*^{R} compared to *Ae. aegypti*^{S} can be attributed to differences in innate recognition of filarial pathogens, or is instead regulated by the mosquito commensal load and/or composition.

Silencing of Cactus and Caspar has been previously used to assess mosquito–parasite interactions (29, 46–48). In contrast to what we show here, one study reported that artificial activation of Toll signaling did not change the number of *B. malayi* larvae developing in the thoracic flight muscle (19). There were two major differences between that study and ours. First, we injected dsRNA after the mosquitoes were infected, whereas the previous study injected the mosquitoes beforehand. Given that RNA interference is transient, a difference in the timing of gene silencing relative to filarial infection might have contributed to the different outcomes. Second, we performed an assay for transmission-stage larvae, the final stage of development in the mosquito that can be assayed. The previous study assayed intermediate stages of the *B. malayi* lifecycle (second- and third-stage larvae) and found that larval numbers were not different. In fact, their finding is consistent with our observation that activating Toll signaling only suppresses development of transmission-stage *D. immitis* but does not alter the total number of larvae. As our emergence assay specifically quantifies infectious third-stage larvae, it more directly assesses transmission efficacy and, as it is more demanding on the parasites, is likely to be more sensitive to subtle differences. While we use the assay on individual mosquitoes, this same assay can be performed on large groups of mosquitoes en masse, making it attractive for detecting transmission-stage filarial larvae in field populations of mosquitoes.

Malpighian tubules have been suggested as a novel target for mosquito control via mosquitocides that specifically target renal function in hematophagous females (49). Our work suggests that they could also be a target for control through a tissue-specific expression system targeting immune up-regulation. Our work raises the possibility that genetically engineered mosquitoes could be used to block filarial worm transmission. Overexpression of Rel2, the IMD pathway-specific NF-κB transcription factor, in *Anopheles stephensi* using a blood meal-responsive and tissue-restricted promoter blocks development of malaria parasites without imposing significant fitness costs (50, 51). To adopt this approach to block transmission of filariae, an appropriate promoter will need to be identified. However, it first must be determined whether ds*Cactus* treatment directly activates immunity in the tissue in which larvae develop, or whether the boost in immune responsiveness occurs as an indirect result of ds*Cactus*-mediated immune activation in other tissues and cells, such as the mosquito fat body and hemocytes (*SI Appendix*, Fig. S9). For example, in *Anopheles gambiae*, Toll signaling increases the number of hemocyte-derived microvesicles found in midgut cells infected by *Plasmodium berghei* (46). If this mechanism is conserved in *Aedes*, then it is possible that the elevated immune response triggered by ds*Cactus* might be due to the association of hemocytes or hemocyte-derived microvesicles with the infected Malpighian tubule cells. Furthermore, infection of *Drosophila* by the nematode *Heterorhabditis gerrardi* results in reduction of Transforming Growth Factor beta expression (52). In support of the idea that secreted products could inhibit larval development, hemolymph transfer from refractory to susceptible *Ae. aegypti* demonstrated that refractory hemolymph is inhibitory to development of *B. malayi* (53). Regardless of whether larvae are restricted autonomously by activation of Toll signaling in their site of development or by activation of Toll signaling in another tissue, existing suitable tissue-selective expression systems for fat body (26) or indirect flight muscle (54), or newly generated expression systems for the Malpighian tubules identified using the transcriptomic information generated in this study and others (55), could be used to promote tissue-specific activation.

Treatment of humans with lymphatic filariasis and dogs with canine heartworm disease is logistically and economically challenging. Developing refractory transgenic mosquitoes using self-propagating genetic drive systems potentially addresses these hurdles and could contribute to current efforts to reduce pathogen transmission and, ultimately, disease burden. Any transgenic approach targeting filarial vectors would need to take into account other human pathogens they transmit. Our work highlights the mosquito immune system as an attractive target for such transgenic approaches.

Materials and Methods

Mosquito Strains. *Ae. aegypti* strains were provided by the NIH/National Institute of Allergy and Infectious Diseases (NIAID) Filariasis Research Reagent Resource Center for distribution by BEI Resources, NIAID, NIH. *Ae. aegypti*^{S} (*Ae. aegypti*, Strain Black Eye Liverpool, Eggs, NR-48921) is a *D. immitis*- and *B. malayi*-susceptible strain. *Ae. aegypti*^{R} (*Ae. aegypti*, Strain LVP-IB12, Eggs,

MRA-735, contributed by David W. Severson, University of Notre Dame, Notre Dame, IN) is a *D. immitis*- and *B. malayi*-refractory strain. Both strains were reared at 27 °C and 80% humidity with a 12-h photoperiod. Mosquitoes were housed in 30-cm^3 cages (Bugdorm) at a density of ≤1,000 per cage. Larvae were maintained at a density of 1 larva per 3 mL. Larvae were fed a suspension of liver powder in water (MP Biomedicals), and adults were maintained with 10% sucrose in water. Heparinized sheep blood (Hemostat) was provided using an artificial membrane feeder at 37 °C for egg production.

Mosquito Infection. Blood containing *D. immitis* microfilariae (mf) was obtained from an experimentally infected dog. The experimental dog was established by subcutaneous injection of 30 emerging transmission-stage larvae in 0.5 mL of saline. Transmission-stage larvae were isolated en masse from a group of ∼200 *Ae. aegypti*^{S} 17 d after infection with blood containing 3,250 mf per mL obtained from a naturally infected shelter dog in Charleston, NC. The average microfilaremia of the experimental dog during these experiments was ∼50,000 mf per mL. All animal studies were performed under Institutional Animal Care and Use Committee approved protocols and in accordance with the guidelines of the Institutional Animal Care and Use Committee of the University of Pennsylvania (protocol 805059). Blood containing *B. malayi* microfilariae (*B. malayi* microfilariae in cat blood, live, NR-48887) was obtained from an experimentally infected cat containing ∼12,000 mf per mL provided by the NIH/NIAID Filariasis Research Reagent Resource Center for distribution by BEI Resources, NIAID, NIH. In both cases, blood was diluted with the appropriate volume of heparinized sheep blood (Hemostat) to a concentration of 3,000 to 4000 mf per mL. Blood containing microfilariae was warmed to 37 °C and placed in an artificial membrane feeder consisting of the indentation in the bottom of a 300-mL plastic baby bottle (Phillips Avent) filled with 37 °C water. The blood was then covered with thinly stretched Parafilm. The bottle was inverted, placed on top of netted mosquito cups, and removed after 20 min. The indentation holds ∼3.5 mL of blood, resulting in an average uptake of 14 mf per mosquito (range 5 to 24 mf per mosquito) for *D. immitis* and 9 mf per mosquito (range 2 to 19 mf per mosquito) for *B. malayi* at the concentration used. Immediately following the feed, blood-fed mosquitoes were separated using CO_2 anesthesia.

Assaying Filariae. Uptake of microfilariae was measured within an hour of blood feeding. The blood-filled midgut was dissected in water and immediately transferred intact to a glass slide with a 50-μL drop of water. The midgut tissue was disrupted, allowing the water to penetrate into the compacted blood. After a 5-min incubation, the drop was pipetted to disperse the material, while carefully avoiding air bubbles. The slide was immediately scored without a coverslip for microfilariae, which are easily identifiable following red blood cell lysis by water and conspicuous among the debris given their movement.

Larvae were scored in dissected Malpighian tubules either live-mounted in phosphate-buffered saline (PBS) on a glass slide affixed with a coverslip or after 45-min fixation in 4% formaldehyde made in PBS. Following fixation, tubules were washed three times with PBS and stained with 2 μg/mL Hoechst 33342 (Invitrogen) in PBS for at least 30 min before they were washed again in PBS and mounted in 20 μL of Fluoromount-G (SouthernBiotech) and sealed with a 22-mm square coverslip.

Transmission-stage infectious larvae capable of emerging from mosquitoes were assayed at day 17 postinfection for *D. immitis* and day 12 postinfection for *B. malayi*. Assays were performed similarly for both by dousing groups of mosquitoes in a small plastic strainer in 70% ethanol for 2 min and then washing them through two changes in water before placing mosquitoes individually into wells of a 96-well plate containing 200 μL of Dulbecco's Modified Eagle Medium (DMEM). Each well was inspected under a dissecting microscope to confirm that the proboscis of the mosquito was in contact with the medium. The plate was warmed to 37 °C for 2 h. The number of emerged worms per mosquito was assayed by scanning each well at 4× on an inverted phase-contrast microscope. In some experiments, following the whole-mosquito emergence assay, Malpighian tubules were dissected in PBS and scored live as described above. During the dissection, the head and the carcass were placed into wells of a new 96-well plate in 200 μL of DMEM in the same sequence as in the first assay. Dissected heads and carcasses were treated and scored similarly to intact mosquitoes. Occasionally, an L3 larvae was observed during the dissection and was included in the head and carcass sample.

Gene Silencing. *Ae. aegypti Cactus* (AAEL000709), *Caspar* (AAEL027860), *Rel1* (AAEL007696), and *Rel2* (AAEL007624) were silenced in *Ae. aegypti*^{S} mosquitoes using standard protocols for dsRNA production and gene knockdown. In brief, long dsRNAs corresponding to each target gene were synthesized by PCR amplification of a DNA template from *Ae. aegypti* complementary DNA using primers containing T7 RNA polymerase binding site adapters on both ends (*SI Appendix*, Table S1). GFP was used as a control and was amplified using a plasmid template containing the GFP coding sequence. The DNA product was purified and used as a template for an in vitro transcription reaction (HiScribe T7; NEB) yielding dsRNA. The dsRNA was purified and concentrated to 3 μg/μL, and 69 nL was injected into the mosquito hemocoel. For double knockdown experiments, dsRNA was mixed equally, and 138 nL was injected per mosquito so that they received 69 nL of each dsRNA. The single *Cactus* and *Rel1* knockdown groups in the double knockdown experiment were injected with an equal mixture of the target and control (ds*GFP*) so that they were exposed to the same amount of dsRNA. Similarly, the control in the double knockdown experiment was injected with 138 nL of ds*GFP*. Mosquitoes were injected 4 d prior to injection for experiments testing knockdown prior to infection (*SI Appendix*, Fig. S5), and they were injected immediately following blood feeding otherwise (Figs. 2–4). In the latter case, to make all groups even, all blood-fed, infected mosquitoes were combined before splitting them into individual cups of 65 for injection. For *Cactus* dsRNA treatment groups, two cups of 65 were used to offset the increased mortality. Groups of 5 to 10 mosquitoes were placed into TRIzol (Invitrogen) for analysis of gene silencing by qRT-PCR using the $\Delta\Delta C_t$ method using the primers listed in *SI Appendix*, Table S1. The housekeeping gene, *Ae. aegypti S7* (AAEL009496), was used as a reference for normalization.

RNA Sequencing and Transcriptional Analysis. Malpighian tubules from *Ae. aegypti*^{S} and *Ae. aegypti*^{R} mosquitoes were isolated at day 1, day 2, and day 3 following infection by *D. immitis* and from sugar-fed controls. Malpighian tubules are dissected into PBS by pulling at the last abdominal segment with forceps until the hindgut emerges. Next, the abdomen is opened where it joins the thorax, and the midgut is separated from the thorax. The hindgut, midgut, and Malpighian tubules are removed from the posterior abdomen by pulling again on the previously separated posterior segment with forceps. The hindgut and midgut are separated, leaving a set of tubules. Tubules from five mosquitoes were transferred together to a tube containing TRIzol (Life Technologies) and stored at −80 °C until processing according to the manufacturer's instructions. Purified total RNA was resuspended in water and treated with Turbo DNA-free (Invitrogen) to remove potentially contaminating genomic DNA. The RNA concentration and quality were assayed using a NanoDrop (ThermoFisher), 4200 TapeStation (Agilent), and Qubit 3 Fluorometer (ThermoFisher). Overall, 23 libraries were generated from the 24 conditions, as one replicate of *Ae. aegypti*^{S} control did not yield a sufficient quantity of RNA for library production. Therefore, each condition is from three independent biological replicates, apart from the uninfected baseline control for *Ae. aegypti*^{S}, which is only from two replicates, due to insufficient RNA yield for one replicate. RNA sequencing libraries were prepared using the TruSeq Stranded mRNA Library Prep Kit according to the manufacturer's instructions. Samples were run on Illumina NextSeq 500 using two High Output v2 kit flow cells to generate 75-base pair, single-end reads. Bioinformatic analyses were carried out as previously described (56). Briefly, data analyses were performed using the statistical computing environment R (v3.5.1), RStudio (v1.1.456), and the Bioconductor suite of packages for R (57, 58). Fastq files were mapped to the *Ae. aegypti* transcriptome (Aedes-aegypti-LVP_AGWG_TRANSCRIPTS_AaegL5.1) obtained from VectorBase using Kallisto (59). Reads were imported, annotated, and summarized to genes using Tximport (60). Approximately 8.5 to 70.6 million reads summarized to the *Ae. aegypti* transcriptome. The median number of transcripts mapped per sample is 36.1 million reads, with an average mapping rate of 76%. A similar protocol was used to identify the number of transcripts aligning to the *D. immitis* transcriptome obtained from WormBase ParaSite (dirofilaria_immitis.PRJEB1797.WBPS12.mRNA_transcripts). Approximately 0.02 to 1.2 million reads summarized to the *D. immitis* transcriptome. The median number of transcripts mapped per sample is 0.07 million reads, with an average mapping rate of 0.5%. For *Ae. aegypti* data, gene counts were filtered to remove unexpressed and lowly expressed (>1 count per million across two or more samples) genes. Filtered data were then scaled using weighted trimmed mean of M values with edgeR (61) and normalized using the voom function of limma (62). The prcomp function was used to perform principal component analyses (PCA) on normalized data, and PCA plots were visualized using R package ggplot2 (63). Differentially expressed genes (DEGs; false discovery rate < 0.05 and absolute log2 fold change ≥ 0.59) were identified using limma (62). Differentially expressed, immune-specific genes were identified by intersecting DEGs with immune gene lists and were visualized in volcano plots using R package ggplot2 (63). A list containing 319 predicted immune genes was obtained from ImmnoDB (23). Heat maps of selected differentially expressed genes were created and visualized using R package gplots (64). GSEA (25) was performed on

normalized data against six lists of *Ae. aegypti* gene sets we curated from previous genomic and transcriptomic studies (Dataset S1). Raw data are available on the Gene Expression Omnibus (GEO, accession number GSE142155) (65) and will also be made available to the community via VectorBase.

ACKNOWLEDGMENTS. This work was supported by a University Research Foundation Grant (URF-2017), intramural funds, and NIH Grant AI139060 (to M.P.). J.B.L. was supported by NIH Grants AI050668 and AI44572. J.Y.K. was supported in part by NIH Grant T35 OD010919 and a grant from Merial. Leslie King and Megan Povelones helped with critical reading and revision of the manuscript.

1. D. D. Bowman, C. E. Atkins, Heartworm biology, treatment, and control. *Vet. Clin. North Am. Small Anim Pract* **39**, 1127–1158, vii (2009).
2. J. W. McCall, C. Genchi, L. H. Kramer, J. Guerrero, L. Venco, Heartworm disease in animals and humans. *Adv. Parasitol.* **66**, 193–285 (2008).
3. M. J. Taylor, A. Hoerauf, M. Bockarie, Lymphatic filariasis and onchocerciasis. *Lancet* **376**, 1175–1185 (2010).
4. T. L. Bancroft, Report LXXXV: Some further observations on the life-history of Filaria immitis, Leidy. *Br. Med. J.* **1**, 822–823 (1904).
5. P. B. McGreevy, J. H. Theis, M. M. Lavoipierre, J. Clark, Studies on filariasis. III. *Dirofilaria immitis*: Emergence of infective larvae from the mouthparts of *Aedes aegypti*. *J. Helminthol.* **48**, 221–228 (1974).
6. T. J. Bradley, J. K. Nayar, J. W. Knight, Selection of a strain of *Aedes aegypti* susceptible to *Dirofilaria immitis* and lacking intracellular concretions in the Malpighian tubules. *J. Insect Physiol.* **36**, 709–717 (1990).
7. W. W. Macdonald, The selection of a strain of *Aedes aegypti* susceptible to infection with semi-periodic *Brugia malayi*. *Ann. Trop. Med. Parasitol.* **56**, 368–372 (1962).
8. L. C. Bartholomay, Infection barriers and responses in mosquito–filarial worm interactions. *Curr. Opin. Insect Sci.* **3**, 37–42 (2014).
9. B. T. Beerntsen, A. A. James, B. M. Christensen, Genetics of mosquito vector competence. *Microbiol. Mol. Biol. Rev.* **64**, 115–137 (2000).
10. B. M. Christensen, Observations on the immune response of *Aedes trivittatus* against *Dirofilaria immitis*. *Trans. R. Soc. Trop. Med. Hyg.* **75**, 439–443 (1981).
11. W. W. Macdonald, The genetic basis of susceptibility to infection with semi-periodic *Brugia malayi* in *Aedes aegypti*. *Ann. Trop. Med. Parasitol.* **56**, 373–382 (1962).
12. W. W. MacDonald, C. P. Ramachandran, The influence of the gene Fm (Filarial susceptibility, *Brugia malayi*) on the susceptibility of *Aedes aegypti* to seven strains of Brugia, Wuchereria and Dirofilaria. *Ann. Trop. Med. Parasitol.* **59**, 64–73 (1965).
13. P. B. McGreevy, G. A. McClelland, M. M. Lavoipierre, Inheritance of susceptibility to *Dirofilaria immitis* infection in *Aedes aegypti*. *Ann. Trop. Med. Parasitol.* **68**, 97–109 (1974).
14. M. V. Talluri, E. Bigliardi, G. Cancrini, Comparative ultrastructural study of *Dirofilaria repens* (Nematoda: Filarioidea) development in susceptible and refractory strains of *Aedes aegypti*. *Boll. Zool.* **60**, 377–383 (1993).
15. M. Vegni Talluri, G. Cancrini, An ultrastructural study on the early cellular response to *Dirofilaria immitis* (Nematoda) in the Malpighian tubules of *Aedes aegypti* (refractory strains). *Parasite* **1**, 343–348 (1994).
16. L. Kartman, Factors influencing infection of the mosquito with *Dirofilaria immitis* (Leidy, 1856). *Exp. Parasitol.* **2**, 27–78 (1953).
17. J. K. Nayar, J. W. Knight, T. J. Bradley, Further characterization of refractoriness in *Aedes aegypti* (L.) to infection by *Dirofilaria immitis* (Leidy). *Exp. Parasitol.* **66**, 124–131 (1988).
18. D. M. Sauerman, Jr, J. K. Nayar, Characterization of refractoriness in *Aedes aegypti* (Diptera: Culicidae) to infection by *Dirofilaria immitis*. *J. Med. Entomol.* **22**, 94–101 (1985).
19. S. M. Erickson *et al*., Mosquito infection responses to developing filarial worms. *PLoS Negl. Trop. Dis.* **3**, e529 (2009).
20. P. Juneja *et al*., Exome and transcriptome sequencing of *Aedes aegypti* identifies a locus that confers resistance to *Brugia malayi* and alters the immune response. *PLoS Pathog.* **11**, e1004765 (2015).
21. Z. Kambris, P. E. Cook, H. K. Phuc, S. P. Sinkins, Immune activation by life-shortening Wolbachia and reduced filarial competence in mosquitoes. *Science* **326**, 134–136 (2009).
22. C. A. Lowenberger *et al*., *Aedes aegypti*: Induced antibacterial proteins reduce the establishment and development of *Brugia malayi*. *Exp. Parasitol.* **83**, 191–201 (1996).
23. R. M. Waterhouse *et al*., Evolutionary dynamics of immune-related genes and pathways in disease-vector mosquitoes. *Science* **316**, 1738–1743 (2007).
24. V. K. Mootha *et al*., PGC-1α-responsive genes involved in oxidative phosphorylation are coordinately downregulated in human diabetes. *Nat. Genet.* **34**, 267–273 (2003).
25. A. Subramanian *et al*., Gene set enrichment analysis: A knowledge-based approach for interpreting genome-wide expression profiles. *Proc. Natl. Acad. Sci. U.S.A.* **102**, 15545–15550 (2005).
26. Z. Zou *et al*., Transcriptome analysis of *Aedes aegypti* transgenic mosquitoes with altered immunity. *PLoS Pathog.* **7**, e1002394 (2011).
27. J. A. Souza-Neto, S. Sim, G. Dimopoulos, An evolutionary conserved function of the JAK-STAT pathway in anti-dengue defense. *Proc. Natl. Acad. Sci. U.S.A.* **106**, 17841–17846 (2009).
28. E. Rancès, Y. H. Ye, M. Woolfit, E. A. McGraw, S. L. O'Neill, The relative importance of innate immune priming in Wolbachia-mediated dengue interference. *PLoS Pathog.* **8**, e1002548 (2012).
29. L. S. Garver, Y. Dong, G. Dimopoulos, Caspar controls resistance to *Plasmodium falciparum* in diverse anopheline species. *PLoS Pathog.* **5**, e1000335 (2009).
30. A. R. Wattam, B. M. Christensen, Further evidence that the genes controlling susceptibility of *Aedes aegypti* to filarial parasites function independently. *J. Parasitol.* **78**, 1092–1095 (1992).
31. A. R. Wattam, B. M. Christensen, Induced polypeptides associated with filarial worm refractoriness in *Aedes aegypti*. *Proc. Natl. Acad. Sci. U.S.A.* **89**, 6502–6505 (1992).
32. D. Cooper, C. Wuebbolt, C. Heryanto, I. Eleftherianos, The prophenoloxidase system in *Drosophila* participates in the anti-nematode immune response. *Mol. Immunol.* **109**, 88–98 (2019).
33. X. Y. Li, R. S. Cowles, E. A. Cowles, R. Gaugler, D. L. Cox-Foster, Relationship between the successful infection by entomopathogenic nematodes and the host immune response. *Int. J. Parasitol.* **37**, 365–374 (2007).
34. B. M. Christensen, M. M. LaFond, Parasite-induced suppression of the immune response in *Aedes aegypti* by *Brugia pahangi*. *J. Parasitol.* **72**, 216–219 (1986).
35. P. B. McGreevy, "Inheritance of susceptibility to *Dirofilaria immitis* infection in *Aedes aegypti* with observations on the behavior of filariae in refractory mosquitoes" in *Zoology*, PhD thesis, University of California, Davis, CA (1972).
36. P. Oothuman, M. G. Simpson, B. R. Laurence, Abnormal development of a filarial worm, *Brugia patei* (Buckley, Nelson and Heisch), in a mosquito host, *Anopheles labranchiae atroparvus* van Thiel. *J. Helminthol.* **48**, 161–165 (1974).
37. M. G. Simpson, B. R. Laurence, Histochemical studies on microfilariae. *Parasitology* **64**, 61–88 (1972).
38. T. Kaneko *et al*., PGRP-LC and PGRP-LE have essential yet distinct functions in the drosophila immune response to monomeric DAP-type peptidoglycan. *Nat. Immunol.* **7**, 715–723 (2006).
39. J. McGettigan *et al*., Insect renal tubules constitute a cell-autonomous immune system that protects the organism against bacterial infection. *Insect Biochem. Mol. Biol.* **35**, 741–754 (2005).
40. P. Verma, M. G. Tapadia, Immune response and anti-microbial peptides expression in Malpighian tubules of *Drosophila melanogaster* is under developmental regulation. *PLoS One* **7**, e40714 (2012).
41. W. Zheng *et al*., Dehydration triggers ecdysone-mediated recognition-protein priming and elevated anti-bacterial immune responses in *Drosophila* Malpighian tubule renal cells. *BMC Biol.* **16**, 60 (2018).
42. N. Buchon, N. Silverman, S. Cherry, Immunity in *Drosophila melanogaster*—From microbial recognition to whole-organism physiology. *Nat. Rev. Immunol.* **14**, 796–810 (2014).
43. S. A. Davies, J. A. Dow, Modulation of epithelial innate immunity by autocrine production of nitric oxide. *Gen. Comp. Endocrinol.* **162**, 113–121 (2009).
44. S. A. Davies *et al*., Neuropeptide stimulation of the nitric oxide signaling pathway in *Drosophila melanogaster* Malpighian tubules. *Am. J. Physiol.* **273**, R823–R827 (1997).
45. M. Ming, F. Obata, E. Kuranaga, M. Miura, Persephone/Spätzle pathogen sensors mediate the activation of Toll receptor signaling in response to endogenous danger signals in apoptosis-deficient *Drosophila*. *J. Biol. Chem.* **289**, 7558–7568 (2014).
46. J. C. Castillo, A. B. B. Ferreira, N. Trisnadi, C. Barillas-Mury, Activation of mosquito complement antiplasmodial response requires cellular immunity. *Sci. Immunol.* **2**, eaal1505 (2017).
47. C. Frolet, M. Thoma, S. Blandin, J. A. Hoffmann, E. A. Levashina, Boosting NF-kappaB-dependent basal immunity of *Anopheles gambiae* aborts development of *Plasmodium berghei*. *Immunity* **25**, 677–685 (2006).
48. Z. Xi, J. L. Ramirez, G. Dimopoulos, The *Aedes aegypti* toll pathway controls dengue virus infection. *PLoS Pathog.* **4**, e1000098 (2008).
49. P. M. Piermarini, C. J. Esquivel, J. S. Denton, Malpighian tubules as novel targets for mosquito control. *Int. J. Environ. Res. Public Health* **14**, E111 (2017).
50. A. Pike *et al*., Changes in the microbiota cause genetically modified *Anopheles* to spread in a population. *Science* **357**, 1396–1399 (2017).
51. Y. Dong *et al*., Engineered *Anopheles* immunity to *Plasmodium* infection. *PLoS Pathog.* **7**, e1002458 (2011).
52. J. Patrnogic, C. Heryanto, Y. Ozakman, I. Eleftherianos, Transcript analysis reveals the involvement of NF-κB transcription factors for the activation of TGF-β signaling in nematode-infected *Drosophila*. *Immunogenetics* **71**, 501–510 (2019).
53. M. Kobayashi, N. Ogura, H. Yamamoto, Studies on filariasis X: A trial to analyze refractory mechanisms of the mosquito *Aedes aegypti* to the filarial larvae *Brugia malayi* by means of parabiotic twinning. *Dokkyo J. Med. Sci.* **13**, 61–67 (1986).
54. G. Fu *et al*., Female-specific flightless phenotype for mosquito control. *Proc. Natl. Acad. Sci. U.S.A.* **107**, 4550–4554 (2010).
55. Y. Li *et al*., RNA-seq comparison of larval and adult Malpighian tubules of the yellow Fever mosquito *Aedes aegypti* reveals life stage-specific changes in renal function. *Front. Physiol.* **8**, 283 (2017).
56. D. P. Beiting *et al*., Differential induction of TLR3-dependent innate immune signaling by closely related parasite species. *PLoS One* **9**, e88398 (2014).
57. R. C. Gentleman *et al*., Bioconductor: Open software development for computational biology and bioinformatics. *Genome Biol.* **5**, R80 (2004).
58. W. Huber *et al*., Orchestrating high-throughput genomic analysis with bioconductor. *Nat. Methods* **12**, 115–121 (2015).
59. N. L. Bray, H. Pimentel, P. Melsted, L. Pachter, Near-optimal probabilistic RNA-seq quantification. *Nat. Biotechnol.* **34**, 525–527 (2016).
60. C. Soneson, M. I. Love, M. D. Robinson, Differential analyses for RNA-seq: Transcript-level estimates improve gene-level inferences. *F1000 Res.* **4**, 1521 (2015).
61. M. D. Robinson, D. J. McCarthy, G. K. Smyth, edgeR: A bioconductor package for differential expression analysis of digital gene expression data. *Bioinformatics* **26**, 139–140 (2010).
62. M. E. Ritchie *et al*., Limma powers differential expression analyses for RNA-sequencing and microarray studies. *Nucleic Acids Res.* **43**, e47 (2015).
63. ggplot2, Version 3.1.1. https://cran.r-project.org/web/packages/ggplot2/index.html. Accessed 11 April 2019.
64. gplots, Version 3.0.1.1. https://cran.r-project.org/web/packages/gplots/index.html. Accessed 11 April 2019.
65. E. B. Edgerton, C. T. Berry, M. Povelones, Activation of mosquito immunity blocks the development of transmission-stage filarial nematodes. Gene Expression Omnibus. https://www.ncbi.nlm.nih.gov/geo/query/acc.cgi?acc=GSE142155. Deposited 16 December 2019.